GALACSI System Design and Analysis

S.Ströbele*, P.La Penna, R.Arsenault, R.D.Conzelmann, B.Delabre, M.Duchateau, R.Dorn, E.Fedrigo, N.Hubin, J.Quentin, P.Jolley, M.Kiekebusch, J.P.Kirchbauer, B.Klein, J.Kolb, H.Kuntschner, M.Le Louarn, J.L.Lizon, P.-Y.Madec, L.Pettazzi, C.Soenke, S.Tordo, J.Vernet [a]
R.Muradore,[b]
[a] European Southern Observatory; Karl-Schwarzschild-Strasse 2; D-85748 Garching; Germany
[b] University of Verona; Strada Le Grazie 15; Ca' Vignal 2; 37134 Verona (ITALY)

ABSTRACT

GALACSI is one of the Adaptive Optics (AO) systems part of the ESO Adaptive Optics Facility (AOF). It will use the VLT 4-Laser Guide Stars system, high speed and low noise WaveFront Sensor cameras (<1e-, 1000Hz) the Deformable Secondary Mirror (DSM) and the SPARTA Real Time Computer to sharpen images and enhance faint object detectability of the MUSE Instrument. MUSE is an Integral Field Spectrograph working at wavelengths from 465nm to 930nm. GALACSI implements 2 different AO modes; in Wide Field Mode (WFM) it will perform Ground Layer AO correction and enhance the collected energy in a 0.2" by 0.2" pixel by a factor 2 at 750nm over a Field of View (FoV) of 1' by 1'. The 4 LGSs and one tip tilt reference star (R-mag <17.5) are located outside the MUSE FoV. Key requirements are to provide this performance and a very good image stability for a 1hour long integration time. In Narrow Field Mode (NFM) Laser Tomography AO will be used to reconstruct and correct the turbulence for the center field using the 4 LGSs at 15" off axis and the Near Infra Red (NIR) light of one reference star on axis for tip tilt and focus sensing. In NFM GALACSI will provide a moderate Strehl Ratio of 5% (goal 10%) at 650nm. The NFM hosts several challenges and many subsystems will be pushed to their limits. The opto mechanical design and error budgets of GALACSI is described here

Keywords: Adaptive Optics, AOF, GLAO, LTAO, MUSE, Sodium Laser Guide Star

1. INTRODUCTION

GALACSI is developed in the frame of the Adaptive Optics Facility AOF [1]. It has 2 operational modes, in WFM it provides a seeing enhancement by means of ground layer correction and in NFM it provides modest Strehl ratio at visible wavelengths.

In WFM the ain requirement is to increase the ensquared energy (EE) within a MUSE spatial pixel of 0.2" by 0.2" by 2 at 750nm and for seeing conditions from 0.6" to 1.1". This shall be achieved with one tip tilt reference star of magnitude 17.5 or brighter located outside the scientific FoV of MUSE . The EE gain variation within the field shall be less than 15% peak to peak. The performance must be achieved during a 1h exposure time. MUSE is working at visible wavelengths meaning it is also sensitive to the LGS wavelength of 589nm. The maximum LGS background allowed is 200photons/s/arcsecond^2

The faint tip tilt star brightness and Sky coverage of >80% at the galactic pole implies that a LGS AO is required. Only ground layer adaptive correction and positioning the LGS outside the FoV allows to achieve the performance uniformity with one deformable mirror [11]. The 4 LGS are pointed 64" off axis. The corresponding WFSs measure the turbulence in each of the 4 directions. The beam overlap depends on the turbulence layer height and is largest for the Ground layer. The reconstructor estimates the DM command for each WFS and averages them before being applied to the ground conjugated DSM. The averaging of the DSM command from each WFS has the effect that only the correlated part of the WFE is corrected being the one of the ground layer turbulence.

In NFM it is required to provide >5% Strehl at 650nm for 0.6" seeing with a NIR tip tilt source of mag 15 in J-H band

To obtain a near diffraction limited PSF core at 650nm even under very good seeing conditions drives many key AO system parameters like number of actuators of the DSM, number of sub-apertures of the WFS, system update frequencies and LGS launch power. It also requires a dedicated tip tilt and low order sensor dubbed IRLOS.
In NFM the LGSs are pointed 10" off axis. In this configuration the turbulence of the full turbulent air volume along the telescope optical axis is probed. The tomography algorithm estimates the WFE and best correction for the scientific target being on axis. This technique is dubbed Laser Tomographic Adaptive Optics LTAO.

Several key components used by the GALACSI AO system are shared with the other AOF systems GRAAL and possibly ERIS like the 4-LGSs system and the DSM. The Real-time computer RTC and WFS camera are common ESO developments but dedicated units will be built for GALACSI. The RTC will be a dedicated unit based on the SPARTA platform [2] performing the AO camera data handling, centroids estimation and DM command calculation with a latency of less than 200μs at the default AO loop rate of 1000Hz. The reconstruction is based on a Vector Matrix multiplication MVM . SARTA includes also a numerical processing cluster allowing the storage of large datasets of real time data and offline data processing. The WFSs are based on the ESO AO camera [3] with an E2V CCD-220 with 240 by 240 pixels with a pixel size of 24μm. It facilitates an electron multiplication readout register and full frame rate of 1000Hz with a read noise below $1e^-$ rms. The tip tilt sensor will use the AO camera without lenslet array, while for the 4 LGS WFSs a lenslet array with 40 by 40 sub-apertures is placed in front of the CCD. The pixel scale of an individual sub-aperture of the WFS is 0.8"/pixel giving a maximum FoV per sub-aperture of 4.8arc sec. by 4.8arc sec.
The opto- mechanics and Control electronics are arranged on the Nasmyth platform of the VLT UT4 (Figure 1). The GALACSI main assembly is mounted the VLT adapter. IRLOS is mounted to the MUSE fore optics extension beam. One Electronic cabinet on the Nasmyth platform hosts the control electronics for main assembly and IRLOS.

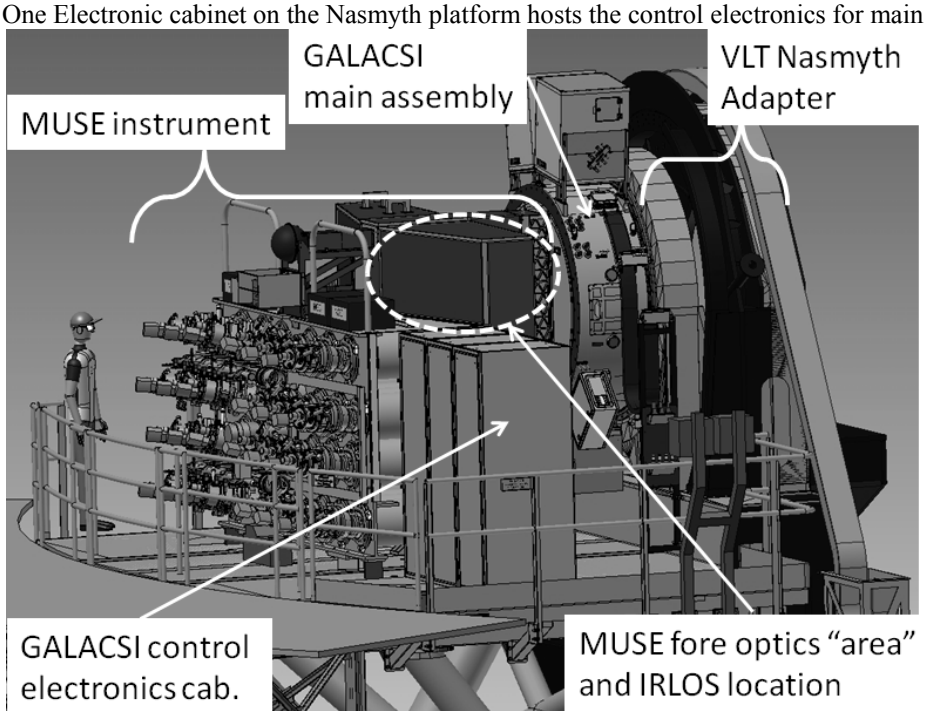

Figure 1 View of the VLT Nasmyth platform. The systems from right to left are: VLT structure (blue) the Nasmyth adapter (grey cylinder), GALACSI main assembly the grey cylindrical structure with red cable guide and attached electronic cabinets and the MUSE Instrument.

2. OPTOMECHNAICAL LAYOUT

GALACSI will be installed on the Nasmyth B platform of the VLT UT 4. It has to share the available space and resources for power supply and cooling with the MUSE Instrument (Figure 1). The main assembly is attached to the Nasmyth rotator and connects via 2 cable chains to its control electronics cabinet Nasmyth platform. The IRLOS assembly is attached to the fore optics extension beam of MUSE. The SPARTA real time computer system [2] the data processing cluster and the servers for the WFS cameras require mainly fiber connections to the WFS cameras and the

DSM. Therefore they were moved to the basement of the UT4 dome. This relaxes constraints on available volume, cooling and vibrations caused by the cooling system.

2.1 Overview on the GALACSI main assembly

The GALACSI main assembly is the cylindrical structure mounted to the VLT Nasmyth rotator. Its opto-mechanical layout is driven by the specifications and opto-mechanical functions to be accommodated.

- 4 High order Shack Hartman sensors based on the ESO AO Cameras [3], a mechanism to compensate the variable focus offset of the LGSs due to their finite distance, 2 stages to change the optical configuration from narrow field mode to wide field mode and one fast piezo tip tilt mirror for each WFS camera to stabilize the LGS images.
- 1 Tip tilt sensor being a ESO AO camera without lens let array
- Tracking field selector to follow the rotation of the tip tilt star
- Calibration unit simulating point sources for field selector and WFS calibration moveable in the field and focus
- Commissioning camera with sufficient field coverage and pixel size to allow a performance measurement. It includes a focusing stage, the possibility to change the plate scale and a filter wheel.
- Beam splitter on a translation stage to send part of the light to the commissioning camera
- Lids or shutters to close the openings of the GALACSI main assembly when it is not used to minimize dust contamination
- All optics to allow the beam shaping and guidance together with the mounts and alignment mechanisms.

The arrangement of the different subsystems is explained with the simplified sketch of the optical design of Figure 2.

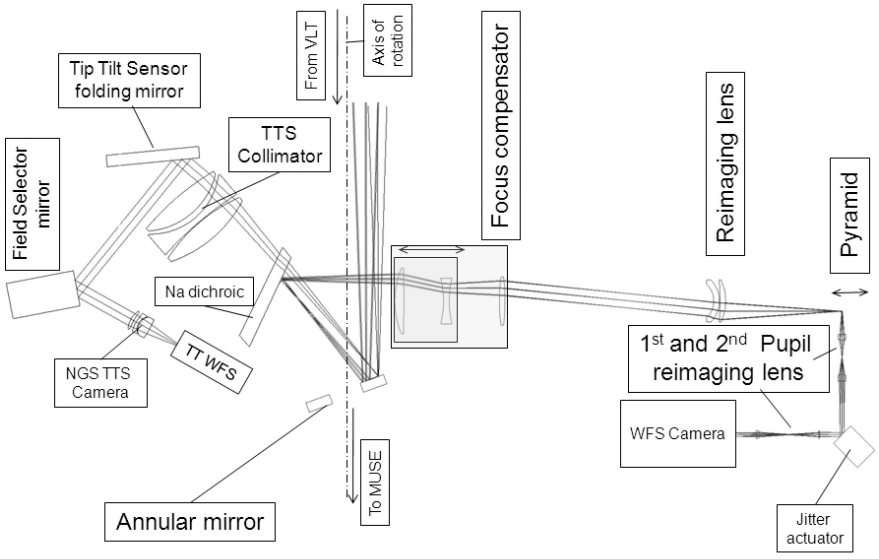

Figure 2 Layout of the optical trains to the Tip tilt sensor and one of the 4 LGS WFSs

The light from the VLT entering from the top in Figure 2 is separated at the Nasmyth focal plane by an annular mirror letting pass the central 1' to MUSE without any light loss and reflecting the light in an annular field of 3.6' outer diameter towards the sodium (Na) dichroic mirror. It reflects the 589nm LGS light towards the LGS WFSs path and lets pass all other wavelength to the tip tilt sensor path. On the TTS path a large collimator forms a pupil where beam steering mirror dubbed field selector is placed. It allows to precisely direct part of the TT FoV to the TTS camera forming an Image on one ESO AO Camera. The pixel scale is 0.167" leading to a maximum FoV of 40". In Closed loop operation only a small window with 3" by 3" around the tip tilt star will be used.

The position of the LGS outside of the scientific FoV helps in reducing the sky contamination by LGS scattered light. To further damp the scattered LGS light it is foreseen to place a notch filter in the MUSE fore optics.
On the LGS path a Focus compensator corrects the LGS focus variation and produces a pupil with a collimated beam at a fixed location. The reimaging lens forms an image plane where a reflective pyramid sends the beams of the 4 LGSs to the corresponding optical trains. Only one of them is shown in Figure 2. Two sets of relay lenses form first an

intermediate pupil image on a PZT tip tilt steerable mirror used to stabilize the LGS image and then to the micro lens array of the SH WFS camera.

For the calibration of the Field Selector and the measurement of the reference slopes of the WFSs several point sources are needed to simulate NGSs and LGSs. As the focal plane is embedded between optical components There is no space to place e.g. fiber point sources directly in the focus, hence a reimaging objective is required dubbed Calibration unit in Figure 3. It images fibre tips of different size arranged on a plate to the Nasmyth focal plane with beam characteristics closely matching the one of the VLT. The light of the Calibration sources can be fed into the system by inserting the CU folding mirror into the entrance beam path.

The commissioning camera is placed at the side of GALACSI where the beam exits the assembly. This avoids obscuration and allows to use and test GALACSI the same way as this is done during normal operations. A beam splitter can be moved into the beam path directing part of the light towards the Commissioning Camera assembly assembly.

In Figure 2 the WFM configuration is shown. To switch to the NFM configuration the LGS are pointed to 10" off axis e.g. their respective beams fall onto the central hole of the annular mirror. This requires the insertion of a dichroic mirror into the hole of the annular mirror, the NFM dichroic. It reflects the LGS light via the Na dichroic towards the LGS optical path as in WFM and transmits the light in the wavelength range from 465nm to 1800nm. For tip tilt and focus sensing the NIR light in the wavelength range from 950nm to 1800nm is separated by a dichroic and sent to a 2x2 sub-aperture SH sensor dubbed IRLOS attached to the fore optics assembly of MUSE (Figure 7).

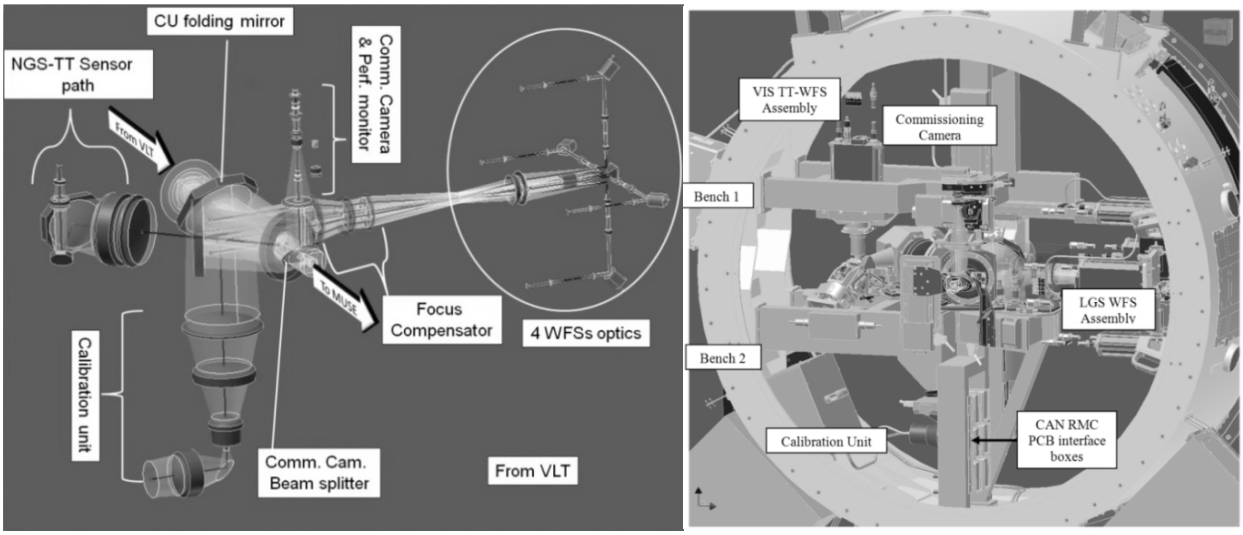

Figure 3 Axonometric views of the optical components of the GALACSI main assembly (left) and a view showing also the structure and all opto-mechanical assemblies

Key sub systems are described to more detail in the following sections

2.1.1 Field Selector

The Field Selector of GALACSI has some particular requirements. For a key science case the exposure time and background of MUSE may not be impacted by light pollution from tip tilt stars. The transmission to MUSE is also a very critical parameter. Therefore we can use only off axis tip tilt stars located outside the MUSE field and within an annular surface. To maintain a constant registration between the patterns of the WFS sub-apertures and the Actuators on the DSM the GALACSI main assembly co-rotates to the Pupil. For a Nasmyth instrument this means to follow the motion of the VLT altitude axis. This has the consequence that as seen from the GALACSI the tip tilt star follows a circular trajectory with the rate of the paralactic angle. To keep the image in a stable position the FS needs to track precisely. The FS is a steering mirror in a pupil. The circular trajectory of the TTS is approximated by the mechanical realization shown in Figure 4. The radial stage points to the radial distance between the field center and the TTS. A rotary stage points to the position angle and performs most of the tracking motion. Because of the beam incidence angle at the field selector of 45˚ the calculation of the actual position command of the FS stages requires a precise

knowledge of the 3 dimensional orientation of the optical axis of the incoming beam, of the rotation axis of the FS turn table and the angle reflected beam. To meet the required specification for the pointing accuracy of the field selector the angles needs to be known with an accuracy of 15".

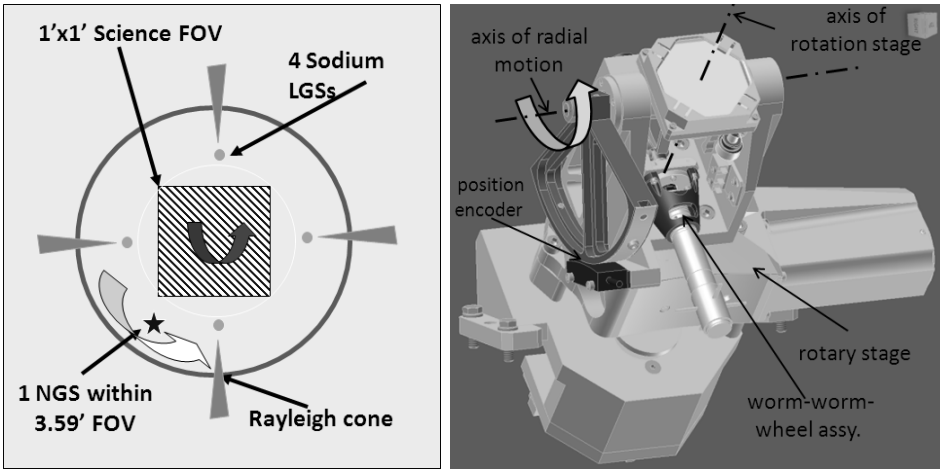

Figure 4 Left: sketch of the image plane arrangement in WFM with the MUSE field, TTS field and LGS locations. Right Field Selector assembly.

2.1.2 Calibration unit

The calibration unit provides point sources for the calibration of the different sub systems:

- 60 Multi mode fibers with 0.12" size, arranged in a rectangular grid covering the full 3.6' Fov of the TTS path. They are used for field selector calibration
- One Fibre for each LGS WFS in WFM and NFM configuration with 1.2" size
- One fibre at the field center with a core diameter of 0.012" to create a sub diffraction limited point source for PSF calibration and suitable to measure the Strehl ratio e.g. on IRLOS and the Commisioning Camera.

The light injection into the fibres is done in a separate housing where the filament of a halogen lamp is imaged on the fibre tip. The intensity of the lap can be SW controlled or adjusted by the insertion of filers and attenuators.

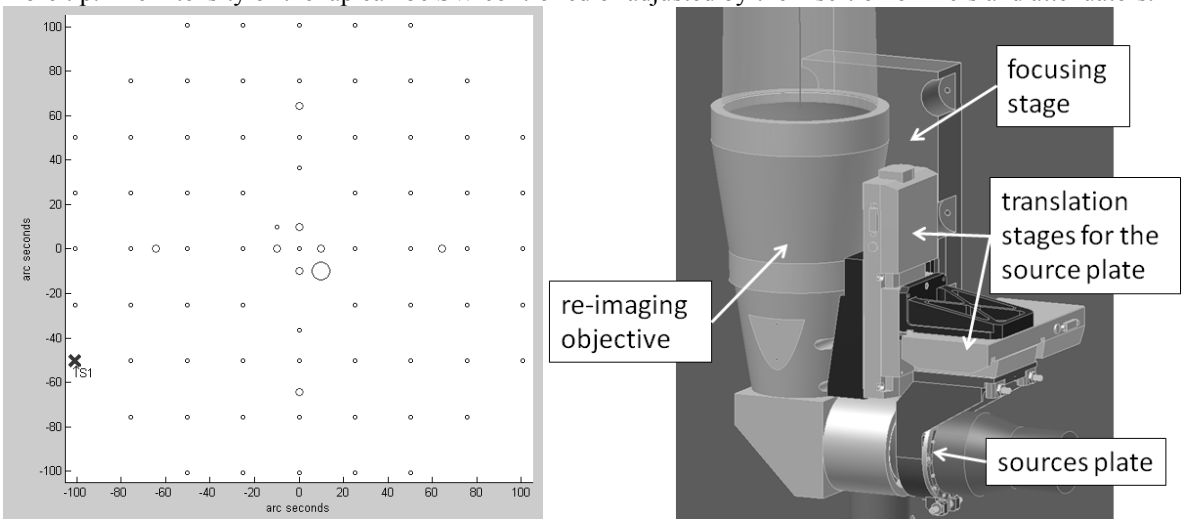

Figure 5 Left: Arrangement of the different point sources of calibration unit. Right: Calibration unit assembly

2.1.3 Focus Compensator

For a multi LGS AO system with several LGS WFSs one has the problem that the LGS focus due to its finite distance and the change of Zenith distance has to be compensated for each of them. Additionally in the case of GALACSI the configuration changes between 2 operational modes. An implementation with classical trombones would require 4

moving functions and numerous optical components. Seeking an alternative B.Delabre came up with an 3 element optical system with one moveable group of 2 lenses. The moveable group follows the LGS focus variation and provides a collimated beam and an exit pupil at a fixed location. The system works regardless of the field position of the LGS. It allows any configuration of the LGSs and in principle also any number of LGSs. To separate the beams and direct them towards the 4 WFSs a reflecting 4 sided pyramid is in an image plane after the focus compensator. The separation of the individual LGSs beams in the LGSs focal plane gives the possibility to position them with only few arc-seconds separation without the risk of light confusion. Using only one focus compensation device cannot correct focus variations of individual LGSs e.g. due to small structured sodium layer altitude variations. For GALACSI the position focus compensator will be corrected by the average focus signal measured by the 4 WFSs.

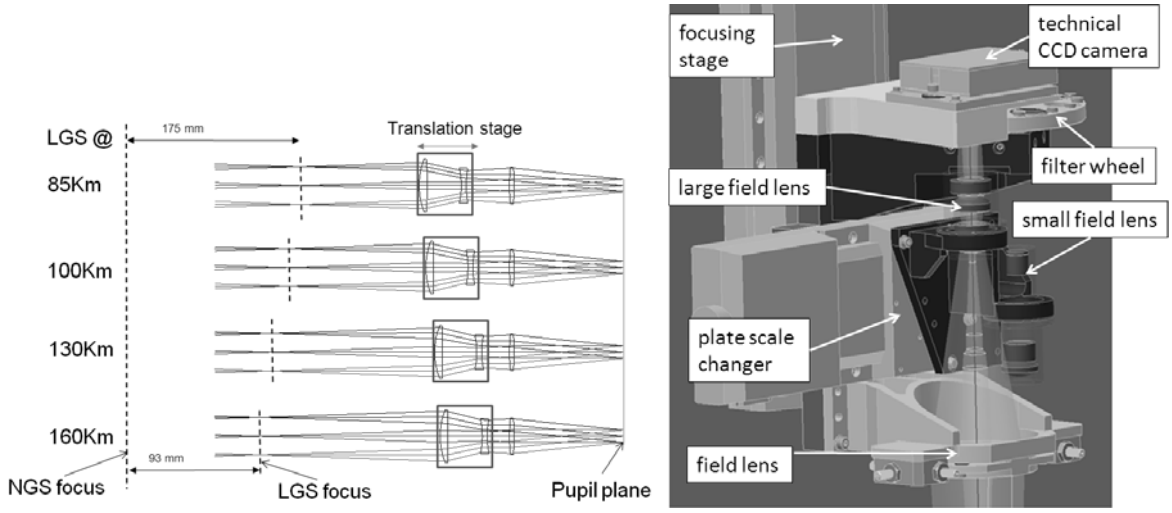

Figure 6: left: Schematics of the Focus compensation system. The ray tracing is shown for 4 different LGS distances covering the operational range from Zenith to 60deg. The LGS light coming from the VLT (further left) focuses 93 to 175mm from the NGS focal plane. The focus compensator forms a collimated pupil with constant size and position by adjusting the position of a 2 elements lens group. Right Commissioning camera assembly

2.1.4 Commissioning Camera

The Commissioning camera is required for a performance verification without the need to reconstruct an image from the MUSE spectra. To do this the camera needs to fulfill the following requirements: Cover the full MUSE field of 1'by1' and to sample the diffraction limited PSF of the VLT at 650nm. The specifications for WFM and NFM are given at different wavelengths. This sets the need for a filter wheel. For the Strehl measurement it is important to have the camera well focused, hence the whole assembly is mounted to a translation stage with sufficient range to also focus the LGSs.
The Camera is based on a ESO Technical CCD camera using a E2V CCD 47-20 chip with 1024 by 1024 pixels. The two pixel scales are 0.082 "/pixel for the large field objective and 0.008"/pixel for the small field lens. The Filter wheel is populated with commercial band pass filters for the specification wavelengths of 650nm and 750nm. Beyond this there is one filter centered at 589nm to improve the LGS visibility and one at 850nm and 940nm for NFM commissioning. At longer wavelength we will get even at slightly worst seeing conditions a near diffraction limited PSF core and will be able to carry out technical tests and performance optimization also under median atmospheric conditions. The camera is mounted to the main assembly of GALCSI and co-rotating to the pupil with the consequence that it suffers field rotation. To avoid image degradation due to the field rotation the maximum exposure time on the largest part of the sky is limited to 5s-10s.

2.1.5 IRLOS

In NFM the NGS must be close to the optical axis and will most of the time be within the scientific field of MUSE, requiring a sensor working at wavelengths outside the ones used by MUSE e.g. NIR light 950nm and beyond. To limit the excessive thermal background beyond the H-band, the detection wavelength range is limited to 1800nm. The key specifications are to provide 5% Strehl (goal 10%) using 1 NGS Star on axis with J-H mag. 15th or to use extended

sources with 3” FWHM. The extended sources can be much brighter. Image drifts caused by IRLOS must be <0.015” per hour of observation. The MUSE pixel scale in NFM is 0.025”and the core of a near diffraction limited PSF core at 650nm is 0.016”. To benefit from the small PSF core, a superb image stability is required implying to implement the tip tilt sensor of the AO system as close to the instrument as practical. This limits the possible sources of differential image motion between IRLOS and MUSE. Therefore the IRLOS assembly is mounted to the Fore Optics beam of MUSE Figure 7. Any differential image motion during an exposure would smear the image and reduce the performance substantially. The main source for differential image motion identified is the MUSE atmospheric dispersion compensator. It cannot perfectly compensate the atmospheric dispersion from 460nm to 1800nm and IRLOS observes the position of a star slightly offset with respect to the location where MUSE sees it. During an observation the offset will change and cause a small relative image drift. It is foreseen to characterize the error and apply an offset to the IRLOS field selector.

The IRLOS assembly includes a filter wheel, a field selector with 10” range and 0.005” accuracy and a plate scale changer carrying 2 optical barrels containing a pupil relay lens and the sup aperture array. The pixel scales are 0.06”/pixel for point sources and 0.25”/pixel for extended sources. The detector is a HAWAI-I detector with 1024 by 1024 pixels and a 4 quadrant architecture. The 4 sub apertures of the lenslet array are arranged such that one SH image falls in each quadrant. The Detector is hosted in a ESO continuous flow cryostat cooled to -190˚C and is controlled by a ESO IR NGC controller. In closed loop operation only 4 small windows around the SH spots will read. 4 windows with 8by8 pixels each can be read at a frequency of 500Hz and a window of 18by18 pixels can be read with 200Hz. The readout noise with double correlated sampling is measured to be excellent at 7e-rms.

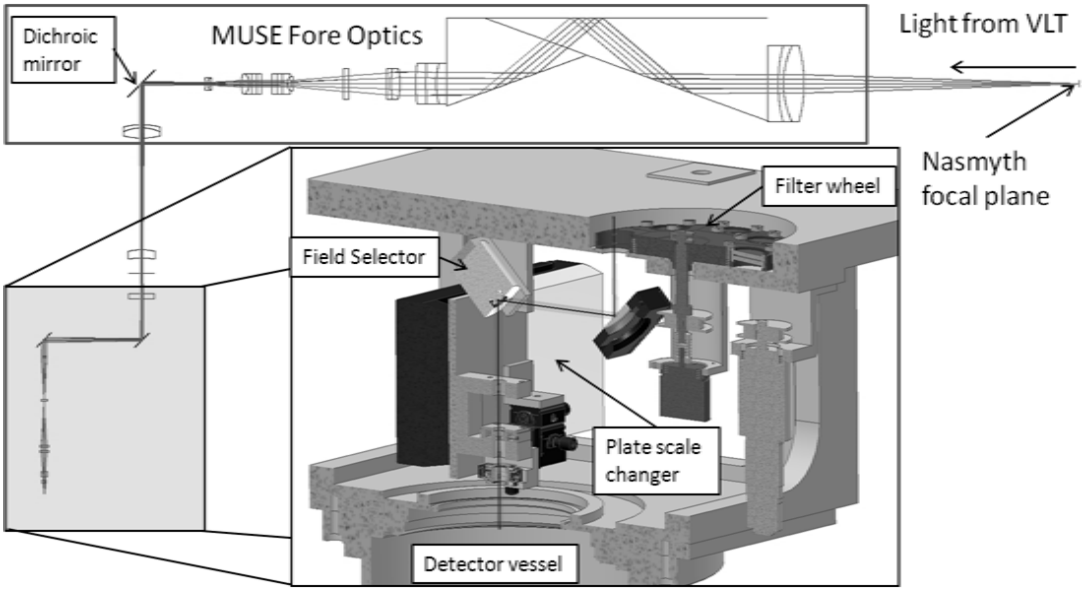

Figure 7: on top is the optical train of the MUSE Fore Optics from the VLT Nasmyth focus (right) to the IRLOS detector. At bottom is an axonometric view of the IRLOS assembly showing the filter wheel, a folding mirror, the IRLOS filed selector and the plate scale changing unit with one of the 2 optical assemblies hosting pupil relay and lenslet array. The detector cryostat is mounted to the bottom of the assembly.

3. PERFORMANCE ANALYSIS

The performance analysis bases on a numerical simulation using the OCTOPUS facility at ESO [11] and the application of a system error budget. The nature of the error budgets differ strongly from WFM and NFM. Also the derived performance metrics and performance predictions are different for both modes.

3.1 WFM Performance analysis

In WFM, GALACSI performs a ground layer correction of the turbulence yielding in a improvement of the FWHM and a increase of the ensquared energy. It is expressed in the form of the increase of ensquared energy within 0.2” by 0.2” compared to seeing limited observation. The AO simulations do not take into account the instrumental error

budget like imperfections of the optics flexures and calibration errors. The most dominant errors are summarized below. The corresponding performance loss is expressed as a loss of EE gain.

Table 1: Error budget in WFM

Effect	Relative EE gain loss at 750nm	Comment
Residual optical aberrations focus loop residuals and VLT vibrations	1	Introduced wave front errors 19nm + 71nm + 33 nm = 80nm rms. This is to be compared to an uncorrected residual WFE of the atmospheric turbulence of ~800nm rms (1.1" seeing) . This is clearly negligible.
Pupil mismatch	0.98	Dedicated simulation run on OCTOPUS.
GALACSI Transmission	0.96	Transmission loss of the Notch filter required for the AO operation to block scattered LGS light outside the blocking wavelength.
Atmospheric dispersion	1	Value at 60 deg off Zenith, it causes an increase of the image size of the tip tilt star. An increase of the size also increases the centroiding error and affects the AO system performance. For the specified mag 18 tip tilt star , this does not impact the System performance.
Image Drifts	(0.97)	Originating from FS calibration and tracking errors and instrumental flexures. It is not taken into account as for normal operation the image drifts of GALACSI will be corrected by the MUSE slow guiding system
EE gain reduction factor	0.965*0.98=0.95	

The performance estimated by the system error budget can be directly applied to the outcome of the end to end simulation. It is obvious that instrumental errors do not have a strong impact in the resulting performance. This changes if one analyses the performance for varying seeing conditions and turbulence profiles. Its impact is analyzed and measured as the faction of time for which a certain performance can be achieved.

3.2 WFM Availability

An extensive measurement campaign and data analysis [11] resulted in a good knowledge of the typical turbulence conditions and the probability of occurrence at Paranal. For different seeing bins centered to 0.6" 0.8 " 1" and 1.2" each a turbulence profile with strong, median and weak turbulence content in the ground layer was determined. This leads to 12 different turbulence profiles and the knowledge of the statistical probability of their occurrence, representing the Paranal conditions. Each profile was used for a simulation run with the end to end model.

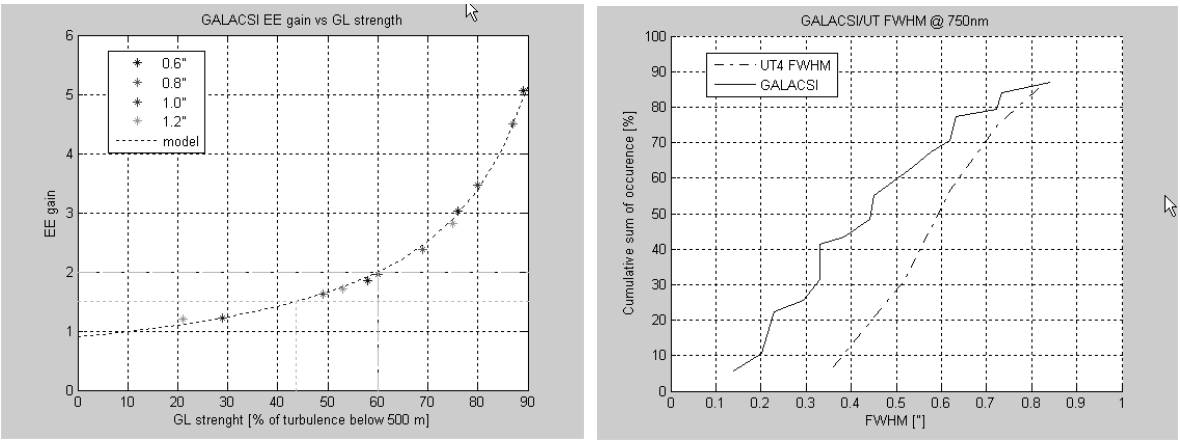

Figure 8 left: Ensquared Energy gain within 0.2"by 0.2" pixels of GALACSI vs. ground layer strength. Right cumulative sum of the occurrence GALACSI provided FWHM compared to the one of VLT UT4 without AO.

The GALACSI performance measured as EE gain for the different conditions versus the fraction of turbulence content in the lower 500m above Paranal is shown (Figure 8 left: Ensquared Energy gain within 0.2"by 0.2" pixels of GALACSI vs. ground layer strength. (Figure 8). The performance metric of Ensquared Energy gain is strongly related to the ground layer strength and can easily be modeled. By the time of the GALACSI commissioning there will be a online monitoring system in operation estimating turbulence strength below 500m. Combining the link between the GL strength and EE gain with an online available measurement of the GL strength allows a simple performance prediction during or even before the start of an observation.

Using the probability of occurrence of the conditions one can also compare the image quality obtained with GALACSI in WFM to the one without (Figure 8 right). It shows the cumulative sum of the occurrence of a given FWHM at 750nm in % of the time for GALACSI and the UT4 without AO. The probability to obtain a very good image quality below < 0.5" FWHM increases substantially. The probability to obtain 0.5" FWHM doubles to 60% of the time and the probability to get 04" triples. The spatial sampling of 0.2" / pixel of MUSE will limit the scientific benefit of the even better image quality occurring occasionally. The % of time used in Figure 8 means clear time i.e.. requires the absence of clouds. The presence of thin clouds will impact the GALACSI operation and with this the availability of the image improvement. Further information on the GALACSI observation planning, preparation and scheduling is given in [11]

3.3 NFM Performance analysis

As already described for WFM the performance analysis in NFM is also based on the numerical model simulated on OCTOPUS. This takes into account the system aspects like DSM and WFS geometries and performance, tomography algorithm and AO loop speed. The key specification is to obtain 5% Strehl (goal 10%) at 650nm for a 0.6" DIMM seeing at line of sight. According to the simulations the PSF will have a very sharp peak embedded in the halo of the uncorrected turbulence. Therefore we can apply to the simulation outcome multiplicative loss values corresponding to the individual contributors of the error budget. They are either derived from the estimated WFE and converted to a relative Strehl loss using the Marechal approximation or originate from sensitivity simulations using the numerical model.

Table 2: Summary of the error budget in NFM. The performance is expressed in a relative Strehl loss at 650nm.

Effect	Rel. Strehl	Comment
Residual optical aberrations	0.76	54nm rms: manufacturing and alignment errors of the components along the WFS optical path. This takes into account that most of the aberrations can be compensated by the measurement of slope offsets for components where the beam footprint does not evolve with the LGS distance. Unfortunately this is not the case for all components. Without offset slopes we expect a rel. Strehl of 0.34 only.
Focus control res.	0.98	Error from IRLOS focus estimate
VLT vibrations	0.90	Systems of the VLT and external disturbances like wind excite vibration modes of some components of the VLT optics causing image jitter at few distinct frequencies. For the analysis we budgeted that the amplitude of the most prominent vibration frequencies can be reduced by a factor 2 [11]
Image drifts from IRLOS instability	0.96	The specification is an image drift of less than 15 mas/hr, here we assume 30min exposure time only, e.g. 7.5 mas pp image motion
WFS Pupil mismatch	0.96	Derived from a sensitivity simulation on OCTOPUS and a budget for pupil registration yielding that the typical mis registration is 12% of a sub-aperture size.
IRLOS Pupil wobble	0.98	Caused by imperfection of the MUSE ADC
Product of the listed reduction factors	0.61	~73 nm rms WFE, or 0.75 relative Strehl at 850nm

The biggest individual entry in the error budget are aberrations of the optics. To a good part this is due to the fact that on some components the beam footprint is changing due to the refocusing to the LGSs. This could be further reduced by measuring slope offsets of the SH sensors with the calibration unit after the telescope preset just before the observation is started. Unfortunately this increases the operational complexity and adds an additional overhead to the

acquisition. As the specification is met there is no strong justification to implement this calibration as a baseline. Image jitter due to vibrations are budgeted to cause a relative performance of 0.90. This can be met only if part of the vibration is rejected. The most prominent vibration frequencies are at 16 and 48 Hz. The baseline update frequency for the tip tilt measurement by IRLOS is 200 Hz. The typical closed loop bandwidth will be around 20Hz and will be not sufficient to correct the vibrations by the normal AO loop. Therefore an adaptive vibration cancellation (AVC) algorithm has been developed in order to cope with structural vibrations that might impact the performance of the AO system. The algorithm proposed performs an on-line estimation of the characteristics of both the perturbation signal and the plant dynamics. On the basis of these estimates, a control signal is generated capable of suppressing vibrations. This approach is capable of coping with a fairly large spectrum of operational conditions requiring minimum operator intervention and is robust against variations in the perturbation signal. Details about the design of the AVC and its expected performance are presented in [12].

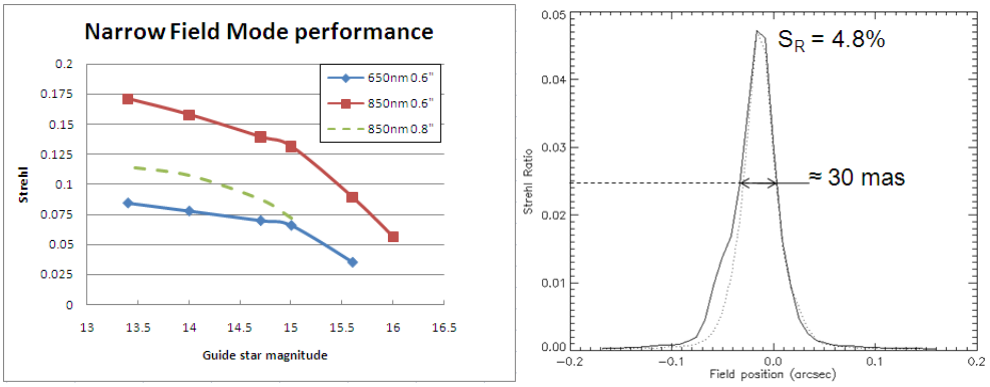

Figure 9: left: NFM AO performance as a function of the TTS magnitude, incl. GALACSI error budget for 650nm under 0.6" seeing and for and 850nm under 0.6" and 0.8 " DIMM seeing. Right: Simulated PSF with typical performance for very faint TTS at 650nm and 0.6" DIMM seeing.

To assess the availability, the sensitivity of the NFM performance was studied. There is a strong link to the seeing. For DIMM Seeing values above 0.8" the central PSF peak essentially vanishes. The NFM performance depends also on the LGS return flux with seasonal and short time variations. For sodium column abundance above 1.6e9/cm^2 the specification of delivering 5% Strehl is met. Even in the season with low abundance 67 % of the time the sodium abundance will be above 1.6e9/cm^2. Thin cloud will likely also prevent the use of NFM. Combining the occurrence of good seeing (~20%) with the Na abundance and clear times gives the estimate that NFM should be useable 10% of the time.

4. STATUS AND OUTLOOK

GALACSI is currently being integrated and tested in the ESO laboratory. By mid 2013 we will finish the optical alignment and subsystem testing. This will be followed by a phase for system level tests including a flexure verification. Beginning 2014 a 6 month period for AO system testing with the DSM on ASSIST are foreseen. The commissioning of GALACSI will happen in the second half of 2014.

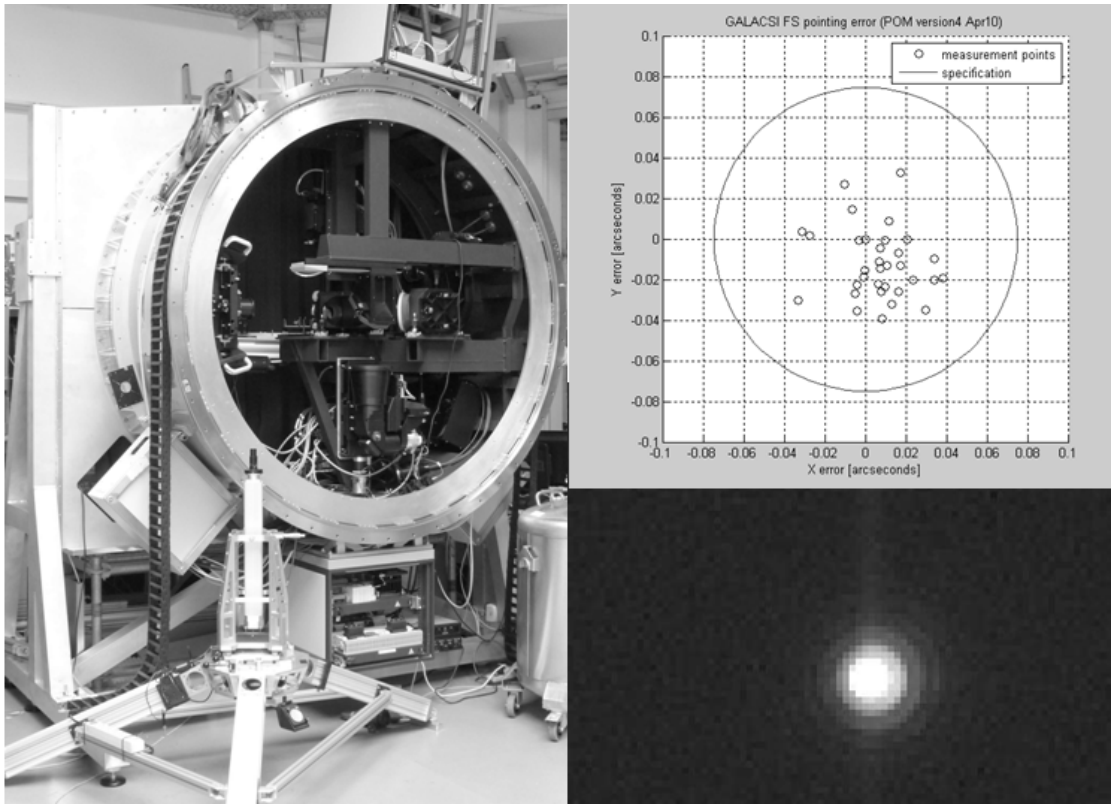

Figure 10 left: GALACSI on its integration stand. Right top: Residual pointing error of the Field Selector after the implementation of a pointing model. Right bottom: Image of a point source taken with the commissioning camera and the 940nm band pass filter to illustrate its optical quality .

REFERENCES

[1] Arsenault, R., et al., "ESO adaptive optics facility", Proc. SPIE 7015, 701524 (2008)

[2] Fedrigo, E., et al., "SPARTA: the ESO standard platform for adaptive optics real time applications", Proc. SPIE, 6272-10 (2006)

[3] Reyes, J., et al., "An overview of the ESO adaptive optics wavefront sensing camera", Proc. SPIE, 8447, 237 (2012)

[4] Paufique, J., Arsenault, R., Madec, P.-Y., et al., "Status of the GRAAL system development: very wide-field correction with 4 laser guide-stars", Proc. SPIE 8447, 116 (2012).

[5] Stuik, R., La Penna, P., Dupuy, C., et al. "Deploying the testbed for the VLT adaptive optics facility: ASSIST", Proc. SPIE 8447, 118 (2012).

[6] Biasi, R., Andrighettoni, M., Angerer, G., et al., "VLT deformable secondary mirror: integration and electromechanical tests results", Proc. SPIE 8447, 88 (2012).

[7] Kuntschner, H., Amico, P., Kolb, J., et al., "Operational concept of the VLT's adaptive optics facility and its instruments", Proc. SPIE 8448, 07 (2012).

[8] Kolb, J., Martinez, P., Girard, J.H.V, "What can be retrieved from adaptive optics real-time data?", Proc. SPIE 8447, 219 (2012).

[9] Kolb, J., Le Louarn, M., Muller, N., et al., "Calibration strategy of the AOF", Proc. SPIE 8447, 85 (2012)

[10] Villecroze, R., Fusco, T., Bacon, R.M., et al., "PSF reconstruction for wide field AO systems: application to the GALACSIMUSE instrument on the VLT", Proc. SPIE 8447, 221 (2012).

[11] Le Louarn, M., et al., "Wide-field adaptive optics for deep-field spectroscopy in the visible", Mon. Not. R. Astron. Soc. 349, 1009-1018 (2004)

[12] Pettazzi,L.,et al., " On the rejection of vibrations in adaptive optics systems", Proc. SPIE 8447, 38 (2012)